

Application of Casting Simulation for Semi-Solid Casting of an Automotive Suspension Component



Winston Sequeira

MAGMA Foundry Technologies Inc.
Arlington Heights, IL

Sean Seaver

SPX Contech
Portage, MI

Presented by:

North American Die Casting Association

This paper is subject to revision. Statements and opinions advanced in this paper or during presentation are the author's and are his/her responsibility, not the Association's. The paper has been edited by NADCA for uniform styling and format. For permission to publish this paper in full or in part, contact NADCA, 9701 W. Higgins Rd., Suite 880, Rosemont, IL 60018-4733, and the author.

Abstract

Semi-solid casting technologies have now emerged as viable and cost-effective ways of manufacturing high integrity near-net shape castings. A variety of semi-solid castings have found their way into automotive applications, primarily in the areas of hydraulics, fuel systems, suspension/steering components and load-bearing structures. Castings that serve these specific applications have to achieve the "holy-grail" quality requirements of superior mechanical properties and zero-porosity. To achieve these objectives within a limited time frame in a product development process, CAD technologies combined with process simulation tools are increasingly used to optimize form filling and solidification of the semi-solid cast parts. This paper discusses a newly developed simulation tool and its application to an automotive suspension component that was prototyped via a semi-solid casting route. Results of semi-solid casting trials showed a high level of confidence in the simulation tools.

Introduction

Even though the semi-solid metal casting process is relatively new, it has now been accepted as a casting process with significant advantages over some other casting techniques. In the main, these advantages include non-turbulent filling of the cavity, low shrinkage in the castings, lower starting temperature of the feedstock and longer tool life. Primarily used for the production of aluminum and magnesium components, market penetration of components manufactured via the semi-solid casting route has increased over the last few years due to several reasons. Of most importance are:

- Wider acceptance that the process has matured and is competitive in a niche market segment
- Assurance that the process will result in components with benchmarked mechanical properties with good process control
- Variants of the process to meet specific demands

- Cost reduction of the semi-solid manufacturing processes
- Better basic understanding of the behavior of the semi-solid processes
- Development of simulation tools to predict cavity filling and solidification

The variants of the semi-solid process and their differences have been discussed in detail elsewhere.¹ This paper deals with the simulation of a high integrity suspension part made via the rheocasting process.

Premise For The Semi-Solid Model Used In The Simulation

The semi-solid material takes advantage of the laminar flow of the material into the die cavity. The semi-solid materials are non-Newtonian fluids, which means that they show a non-linear relationship between the magnitude of applied stress and deformation. Thus, the preconditions for the material used for thixoforming are pseudoplasticity and thixotropy. Pseudoplasticity is the dependence of viscosity on shear rate, and thixotropy means that the stresses in the fluid at any time are not exclusively dependent on its current state of deformation, but also on its recent deformation history. The rheological behavior of the non-Newtonian material governs the way it deforms and flows in response to the applied forces. Viscosity is the most important property that governs rheological behavior. The Ostwald-de Waele model is used to simulate the semi-solid metal flow behavior on the basis of the apparent viscosity plot for a pseudoplastic fluid, shown in figure 1. This plot approximates the pseudoplastic flow behavior into: a) low shear rate -high apparent viscosity regime (lower Newtonian), b) high shear rate -low apparent viscosity region (upper Newtonian) and c) variable viscosity and shear rate region.

Figure 1

Constitutive equations governing the Ostwald de-Waele model are:

Equation 1

Equation 2

Where $\dot{\gamma}$ is the shear rate, m is the time dependent function with dimensions of kinematic viscosity, and n the Ostwald de-Waele co-efficient. For the Ostwald de-Waele thixotropy based model, the calculated values of m and n with temperature are made available, and between certain shear rate limits the simulation tool calculates apparent viscosity and shear stress using the constitutive equations defined by the model. These calculations, combined with a variety of other semi-solid specific thermo-physical inputs, forms the premise for the overall global model used for the simulation of all slurry and semi-solid casting processes.

The Part And Simulation Setup Using MAGMATHIXO

The part illustrated in this simulation study is a steering knuckle for an OEM. The process selected for manufacture of the part was a slurry-on-demand rheocasting process. The aluminum alloy used for the simulation was A357, and the parts were to be heat treated to achieve the benchmarked mechanical properties specified by the OEM. The part and the shot geometry are shown in figures 2 and 3, respectively.

Figure 2

Figure 3

The STL file of the parts, runner, biscuit, die and cooling lines were imported into the simulation tool and meshed. Various entities within the geometry were assigned the appropriate material properties. The details of the die and its cooling circuits are not discussed in this paper. The die was heated to a uniform temperature of 250°C and the initial casting temperature of the alloy slurry was 583°C ($f_s=0.5$). Interfaces between different materials were assigned the correct boundary conditions. After meshing the part and prior to simulation setup, geometry and process listings such as casting volume, gate volume, biscuit volume, total shot volume (poured), gate area, projected area, plunger diameter, shot sleeve length etc. were viewed. Using all the above information, an appropriate shot profile was designed and calculated for the simulation (see figure 4). The higher pouring rate part of the shot profile in figure 4 reflects the higher plunger velocity used to move the slurry near the gate. After the metal reaches the gate, a lower plunger velocity is used during cavity fill.

Results and Discussion

Based on the inputs, several interesting results are obtained during and after the simulation. The simulation yields the following results.

1. Filling of the metal in the runner and the cavity in terms of metal temperature

2. Velocity of the metal in the runner and the cavity
3. Local filling time within the casting cavity
4. Air pressure locations within the casting cavity
5. Solidification results, which include solidification pattern, gate freeze-off, last areas to solidify, Sol-Time, Hot-spot, shrinkage prediction, etc.

Figure 4

The flow rate used for cavity fill during the simulation was a two-stage injection shot profile to displace a charge that was 50 percent fraction solid ($f_s=0.5$). The total shot time was 824 ms. The metal arrived at the gate in approximately 210 ms, and the cavity was filled in 614 ms. The filling of the casting cavity and the related fill velocity at 45 percent shot fill are shown in figures 5 and 6, respectively. Figure 5 shows that the metal was between 583°C - 574°C range, and did not show any significant drop in temperature at 45 percent shot fill. When the shot was 70 percent filled (see figure 7) an overall temperature of 583°C - 570°C was realized and the merging metal fronts moving around the center of the knuckle appeared to contain enough heat content to merge without creating any mending defects. At 45 percent fill, the metal showed a front velocity of approximately 85 cm/sec and a gate velocity in the range 220-245 cm/sec (see figure 6). At 45 percent fill, the metal front appeared somewhat uneven, yet stable. As the filling progressed into the side and the upper arms of the casting, the front velocity increased to 110-140 cm/sec, but no turbulence was observed. The metal then filled smoothly into the cavity until 100 percent filled.

Even though at a macro level the metal appears to flow smoothly, discernable differences in the filling pattern are apparent if the filling results are analyzed in terms of fill time and air pressure results. The fill time results in figure 9 clearly show the local fill time within the casting cavity in seconds. Since the metal arrived at the gate in 210 ms and the whole shot filled in 824ms, the scale is adjusted between these two values so as to reflect the fill time of the knuckle cavity. Ideally, if the metal filled smoothly from the gate to the furthest part of the casting, the color contours would transition gradually from the gate toward the last area to be filled. However, in the case of the knuckle, an area close to the gate with a delayed fill time in the range 560-730 ms was noticed. This area was surrounded by regions having a fill time of 210-250 ms (indicating an earlier fill time). This suggested some backfilling in this area, and a possible chance of some flow-related defect depending on local venting conditions and intensification after cavity fill. Further, correlation to support this view is obtained from the Air Pressure results, which indicates the same area with high air pressure. Other areas in the casting showed even transitions in fill times suggesting that the knuckle filled smoothly.

Air pressure results obtained in the simulation indicate areas in the casting that retain air which should ideally be flushed out of the die via vents on the overflows. In the current simulation, the overflows on the casting were not finalized and were therefore not included in the geometry that was simulated. In fact, one of the aims of the simulation was to identify locations on the knuckle that would need overflows. It was obvious from the orientation of the

geometry in the die that the side and the top arms of the knuckle would be filled last. Hence, during the simulation, vents were placed directly on arms to enable air to escape from the cavity. The air pressure results shown in figures 10 and 11 were obtained after venting the casting via the two arms. Apart from ends of the knuckle arms showing high air pressure (which was expected), several other areas outside and inside the casting showed entrapped air. The air pressure is very qualitative and is mainly a function of metal flow, flow velocity and die venting conditions. It is also a result obtained before the cavity experiences intensification. Hence, the air pressure result must be analyzed and interpreted cautiously, taking into account the final intensification, air pressure location, machining and heat treatment related issues. Another aspect of the air pressure result is that internal areas of the casting may be viewed for air pressure by slicing the casting. An example of this is shown in figure 11 wherein some areas in the casting showed higher internal air pressure because of merging metal fronts during filling. The air pressure values in these areas were in the range of 1100-1500 mbar, which is higher than the atmospheric pressure of 1013 mbar. It has been found that with appropriate venting, air pressure values of greater than 2500 mbar are considered detrimental to casting quality. Investigation of the knuckle casting showed none of the air pressure areas in the casting to be above this critical air pressure limit.

Solidification of the knuckle revealed relatively thick sections of the casting solidifying last. However, they did not reveal feeding or porosity issues for the conservatively predictive criteria functions that were set in the simulation. These functions need fine-tuning for good correlation with actual shrinkage porosity that is found experimentally. Figures 12-14 show solidification results of the knuckle that identify areas in the casting that were likely to show shrinkage porosity. The simulation tool generates more generic results such as Sol-time (see figure 14) and Hot-spot which identify areas in the casting that solidify last and therefore remain as hot spots. Qualitatively, these generic results show areas in the casting, which are likely to result in shrinkage porosity and therefore require special attention and possible intervention. However, whether these areas will definitively result in measurable and qualitative shrinkage porosity requires extensive fine-tuning of these criteria functions. Such prediction will primarily depend on solid/liquid fractions in the charge and the intensification that is used.

Casting trials to produce the knuckle casting were carried out using venting on the two arms as shown in figure 15. These were carried out in a prototype die. Tensile tests were carried out on samples excised from various locations in the casting and these tests conformed to ASTM standards. All these tensile tests were carried out on samples in the non-heated condition. The samples excised from shrinkage-prone areas predicted by the simulation tool failed to achieve the required mechanical properties during testing. However, certain other areas of the casting exceeded the benchmarked mechanical property requirements. Tensile strength of 34.5 ksi, yield strength of 17 ksi and elongation of 6 percent was achieved in these areas. The castings are undergoing detailed metallographic analysis, and the casting process is under further development to manufacture high quality casting with necessary process robustness.

Conclusions

1. The utilization of the simulation tool to carry our filling and solidification analysis on a high integrity part is illustrated. The simulation tool was used to identify overflow locations and filling and solidification related problem areas in the casting.
2. Destructive testing of samples excised from the knuckle showed results that correlated well with the simulation based results.
3. Early analysis of the filling and mold design must be used in identifying problem areas in semi-solid castings.

Figure 5

Figure 6

Figure 7

Figure 8

Figure 9

Figure 10

Figure 11

Figure 12

Figure 13

Figure 14

Figure 15

References

1. W. Sequeira, R. Kind and A. Koch: Development of a Simulation Tool for Thixocasting of Near-Net Shape Parts, Paper No T01-024, 21st International Die Casting Congress and Exposition, Oct 29-Nov 1, 2001, Cincinnati, OH.

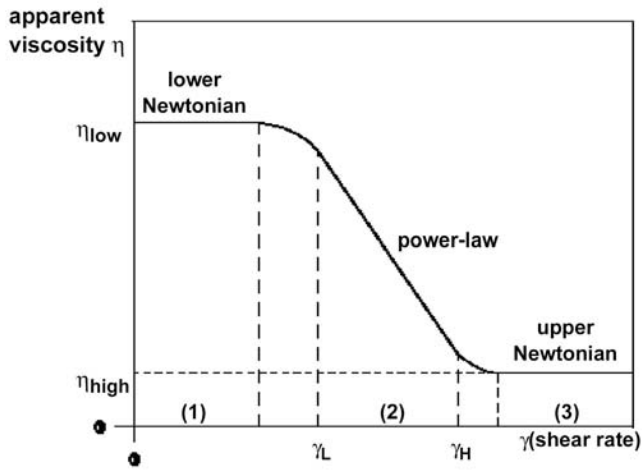


Figure 1 – The apparent viscosity versus shear rate plot used to describe the pseudoplastic behavior of a non-Newtonian fluid.

Apparent viscosity $\eta = \rho.m.\gamma^{n-1}$

Equation 1 –

Shear stress $\tau = \rho.m.\gamma^n$

Equation 2 –



Figure 2 – The geometry of the steering knuckle.

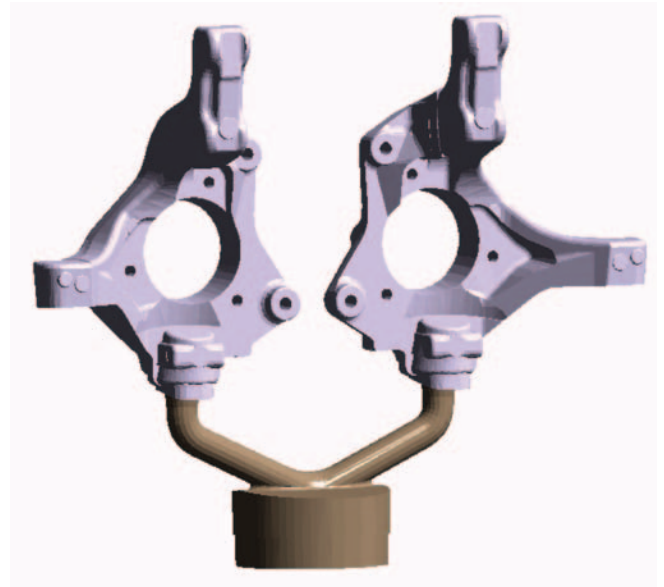


Figure 3 – The two-cavity shot geometry along with runner and biscuit used for the simulation. Since the casting layout was symmetrical in the die, only one half of the shot geometry was simulated.

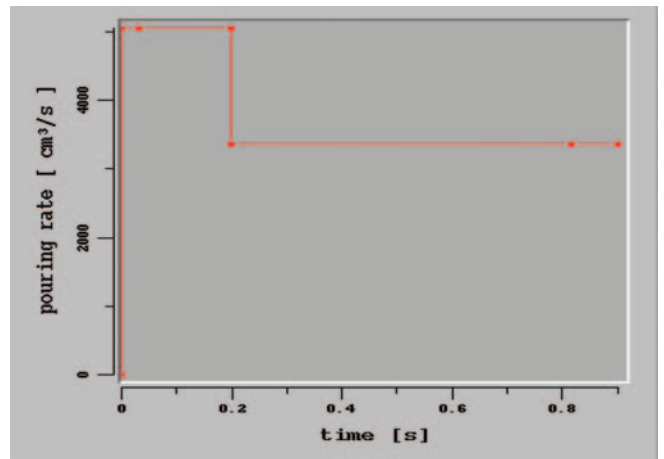


Figure 4 – Shot profile used for the simulation.

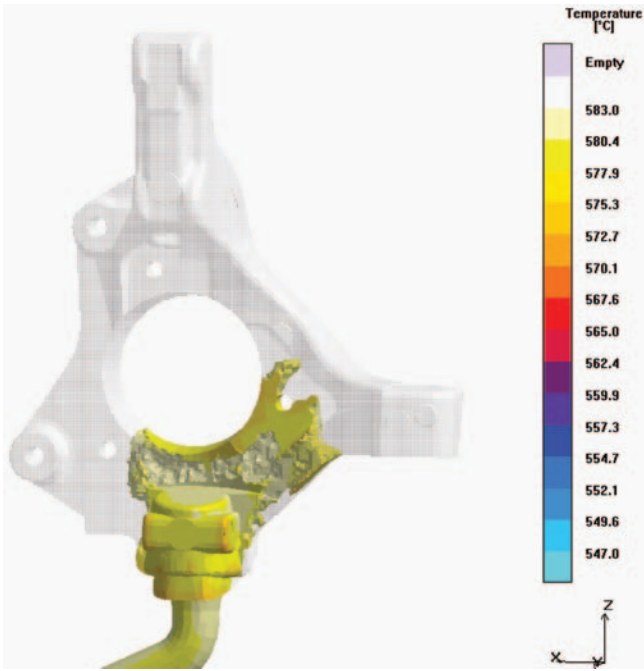


Figure 5 – Filling of the knuckle at 45 percent fill. The scale on the side is between 583°C ($f_s=0.5$) and 547°C (solidus).

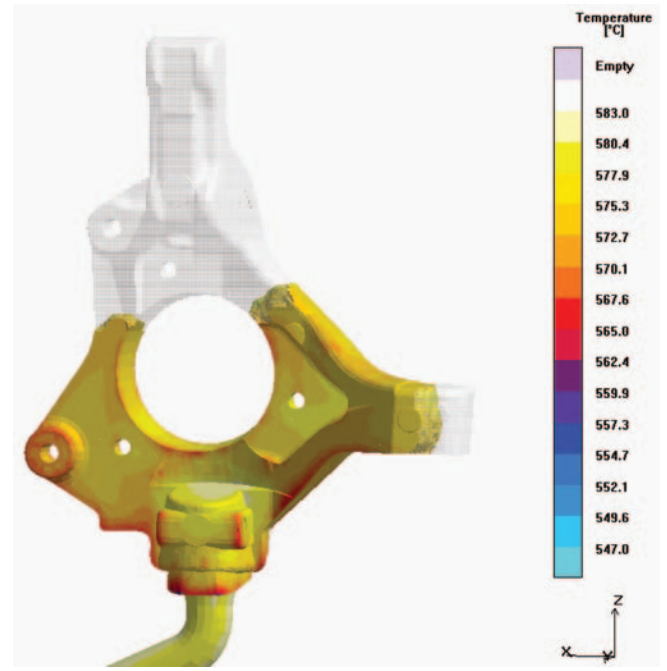


Figure 7 – Filling of the knuckle at 70 percent fill. The scale on the side is between 583°C ($f_s=0.5$) and 547°C (solidus).

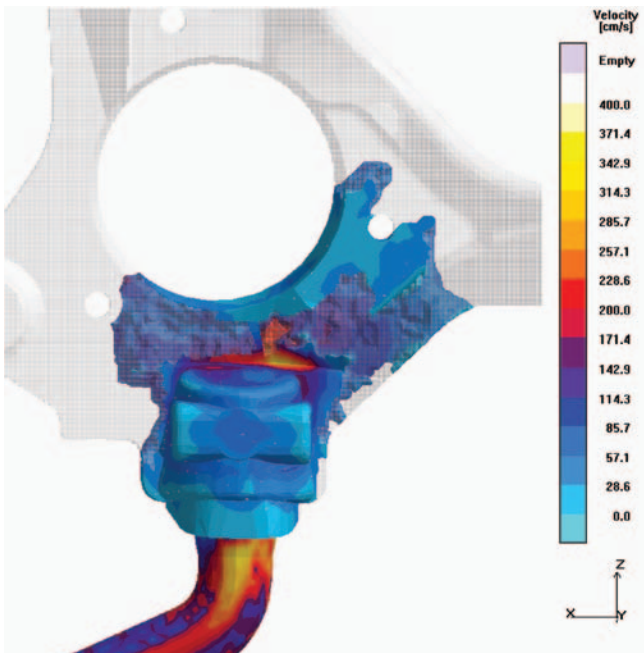


Figure 6 – Fill velocity of the slurry at 45 percent fill. The scale shows a fill velocity between 0 and 400 cm/sec. The fill front shows a velocity of approximately 85 cm/sec and the gate velocity in the range 220-245 cm/sec.

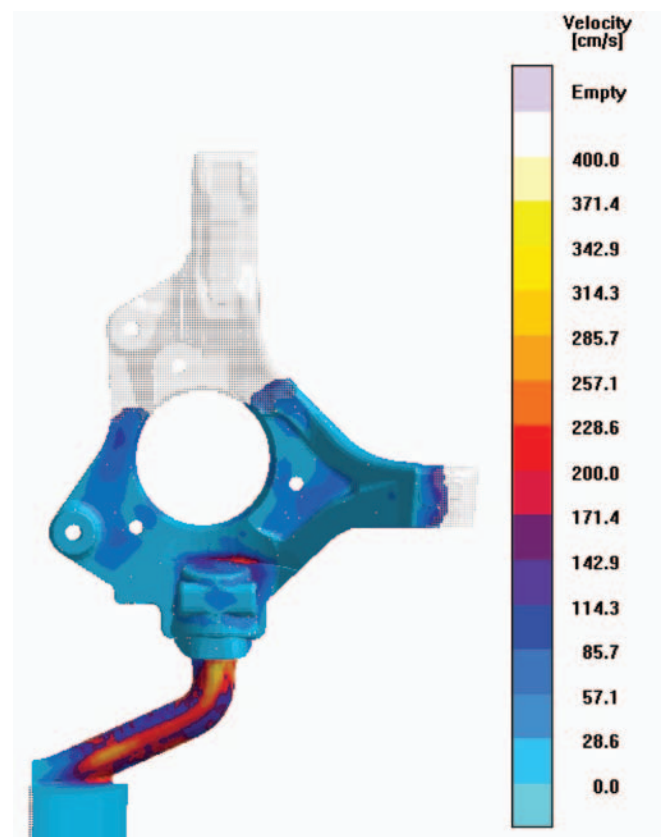


Figure 8 – Fill velocity of the slurry at 70 percent fill. The scale shows a fill velocity between 0 and 400 cm/sec. The fill front shows a velocity of 110-140 cm/sec.

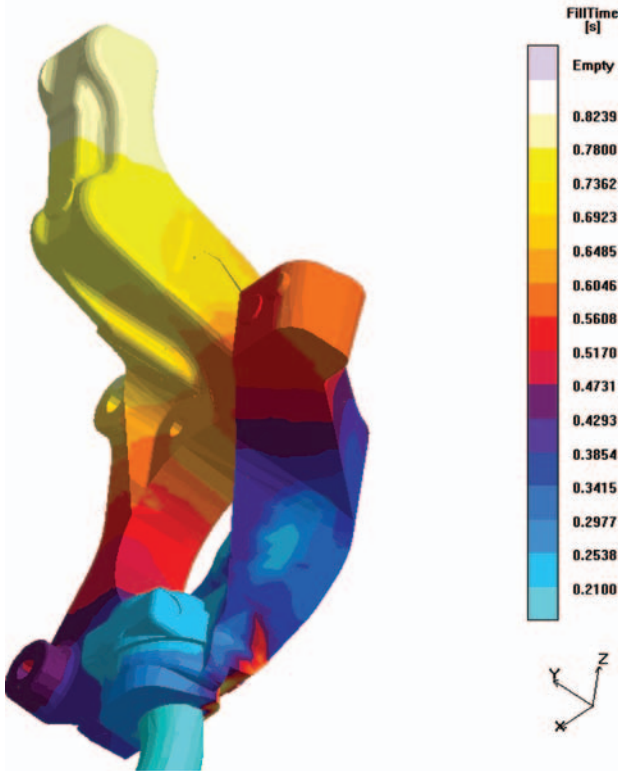


Figure 9 – Fill time result obtained after the cavity was fully filled. The scale reflects a metal-at-the-gate time of 210 ms and 100 percent cavity fill time of 824 ms. An area in the casting close to the gate shows a delayed fill time of 560-730 ms.

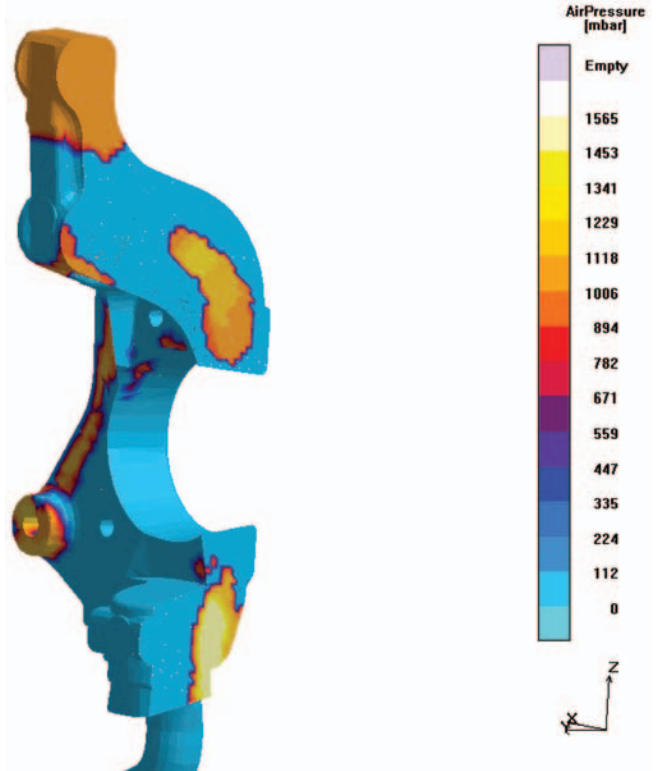


Figure 11 – A section through the casting showing areas inside the casting containing high air pressure. The areas inside the casting show metal fronts enclosing some air during cavity fill.

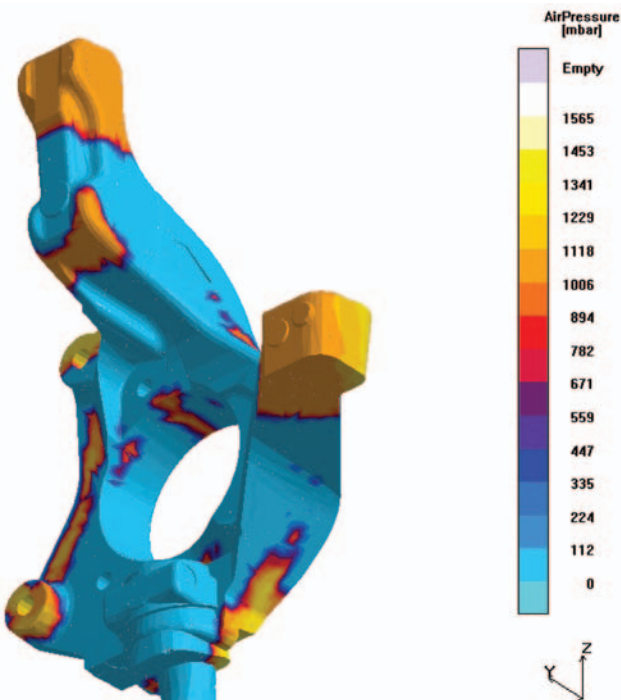


Figure 10 – Air pressure result obtained after the cavity was fully filled. The scale reflects an air pressure in the cavity between 0 and 1565 mbar. Air pressure in the casting above the atmospheric pressure of 1031 mbar is likely to cause fill related porosity.

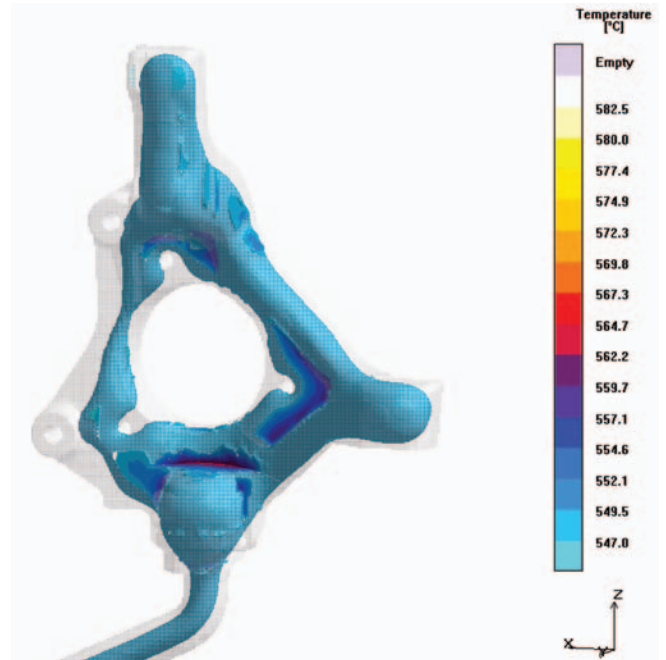


Figure 12 – Solidification of the knuckle after 81 percent fraction solid. The solidified areas of the casting are made x-rayed to show areas that are still in the mushy zone and solidifying last.

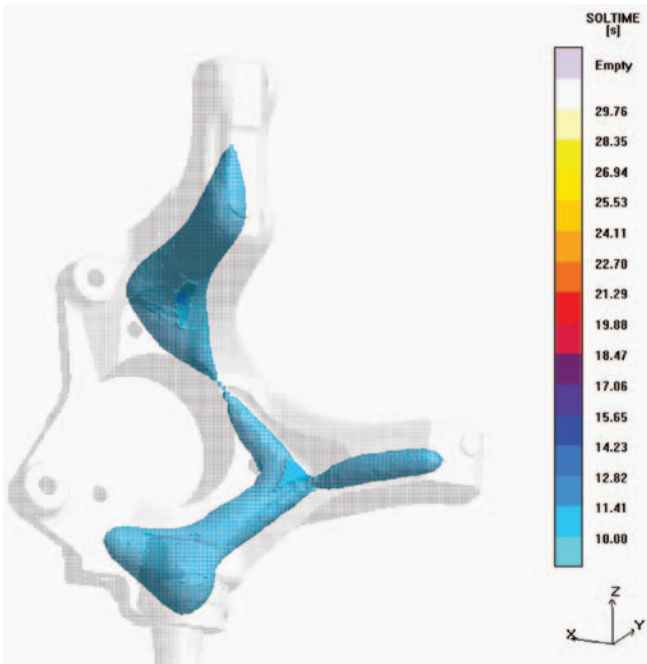


Figure 13 – Solidification of the knuckle after 91 percent fraction solid. Last areas to solidify are clearly visible and areas that are fully solid are x-rayed (to make them invisible).



Figure 15 – Prototyped knuckle casting made via the rheocasting process. Several parts were cast for testing and engineering analysis.

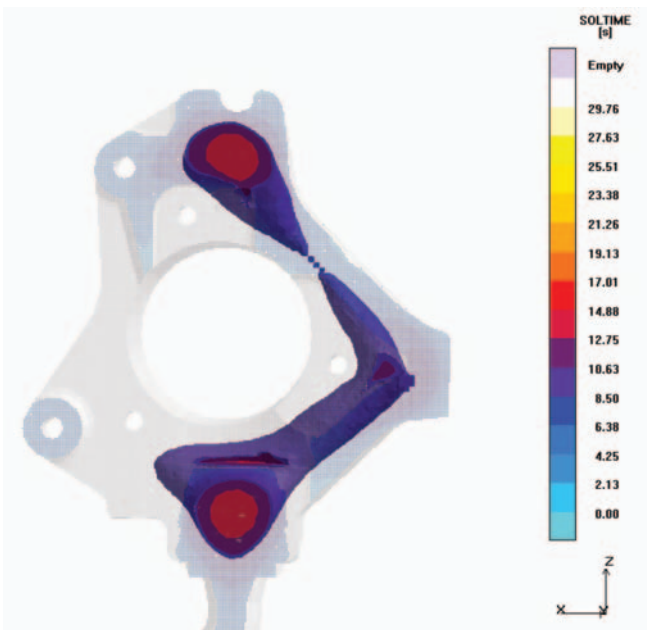


Figure 14 – A slice through the Soltime result. This result shows areas in the casting that solidify last (in terms of time). These are the areas that are likely to show shrinkage porosity.